A shared inhibitory circuit for both exogenous and endogenous control of stimulus selection

Shreesh P Mysore & Eric I Knudsen

The mechanisms by which the brain suppresses distracting stimuli to control the locus of attention are unknown. We found that focal, reversible inactivation of a single inhibitory circuit in the barn owl midbrain tegmentum, the nucleus isthmi pars magnocellularis (Imc), abolished both stimulus-driven (exogenous) and internally driven (endogenous) competitive interactions in the optic tectum (superior colliculus in mammals), which are vital to the selection of a target among distractors in behaving animals. Imc neurons transformed spatially precise multisensory and endogenous input into powerful inhibitory output that suppressed competing representations across the entire tectal space map. We identified a small, but highly potent, circuit that is employed by both exogenous and endogenous signals to exert competitive suppression in the midbrain selection network. Our findings reveal, to the best of our knowledge, for the first time, a neural mechanism for the construction of a priority map that is critical for the selection of the most important stimulus for gaze and attention.

To behave adaptively in a complex environment, an animal must select the most important stimulus at each moment for further neural processing. The selection of the highest priority stimulus for attention is determined by competitive interactions among the neural representations of all stimuli in the environment. Two aspects of each stimulus influence these competitive interactions[1] (also see ref. 2): its physical properties, such as its intensity, speed of motion or novelty, and its relevance to the animal's behavior, such as whether the stimulus predicts reward or whether the animal intends to direct its gaze toward the stimulus. The effects of such exogenous and endogenous influences, respectively, on the neural representations of competing stimuli have been studied extensively in both forebrain (fronto-parietal) and midbrain structures involved in the control of attention, with response suppression being a hallmark of these competitive interactions[3–8]. However, the identity of the neurons that actually mediate competitive suppression is not known.

The midbrain selection network, which is conserved across vertebrate evolution, provides an ideal substrate to search for specific circuits that are involved in stimulus selection[7]. It consists of the optic tectum (superior colliculus in mammals) and a number of interconnected tegmental nuclei that contain groups of GABAergic, cholinergic and glutamatergic neurons. In birds, this network achieves its highest degree of differentiation[7], with functionally distinct circuits being spatially segregated, thereby greatly facilitating the ability to access selectively various network components.

A key node in the midbrain selection network is the intermediate and deep layers of the optic tectum (OTid, layers 10–15 in birds, layers 3–7 in mammals), which is critical for stimulus selection for attention in monkeys[9,10]. The OTid encodes the relative priorities of stimuli for gaze and attention in a topographic map of space by combining multisensory exogenous signals of physical salience with endogenous signals of behavioral relevance associated with each location[7].

Notably, both exogenous and endogenous signals associated with a location competitively inhibit OTid responses to stimuli at all other locations[11–14]. This competitive inhibition results in a highly reliable, categorical representation of the locus of the strongest stimulus, a representation that is exceptionally sensitive to the relative priorities of the competing stimuli[13,15]. Such competitive interactions can account for the correct selection of a target among distractors[16] in behaving monkeys[9,10,16].

What circuit mediates competitive inhibition among exogenous signals, and does the same circuit also mediate competitive inhibition of irrelevant locations by endogenous signals[17]? An obvious candidate circuit in the midbrain network is the Imc (lateral tegmental nucleus in mammals; **Fig. 1** and **Supplementary Fig. 1a**). The Imc is composed of GABAergic neurons that interconnect with the OTid[18]. Imc neurons receive a topographic projection from the OTid (layer 10b) and they project back broadly to the OTid space map[18]. The pharmacology and pattern of connectivity suggest that the Imc may be the source of global inhibition in the OTid. Indeed, Imc blockade has been shown to reduce competitive suppression among exogenous signals in a cholinergic component of the midbrain network[19]. We used reversible blockade of synaptic inputs to the Imc in barn owls to examine the role of the Imc in mediating exogenous and endogenous competitive inhibition in the OTid.
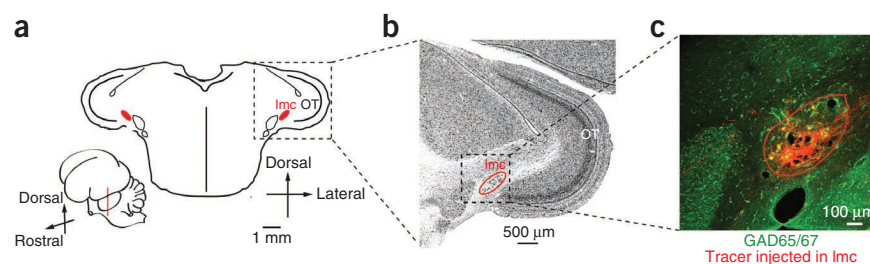
RESULTS

We hypothesized that the Imc mediates the competitive inhibition in the OTid that results from both exogenous and endogenous signals. To test this hypothesis, we measured the strength of exogenous and endogenous competitive inhibition in the OTid before, during and after blocking excitatory synaptic transmission in the Imc in head-fixed, non-anesthetized barn owls. Transmission blockade was achieved by focal, iontophoretic application of kynurenic acid, a competitive

Figure 1 Anatomy of the Imc and optic tectum. (a) Transverse section of owl midbrain showing the optic tectum (OT) and the Imc. Inset, cartoon showing owl brain and plane of section. (b) Nissl stain of the boxed region from a. The optic tectum is the C-shaped, multilayered structure that wraps around the Imc, layer 1 is the outermost layer, layer numbers increase radially inward, and layer 10 is the darkly stained band of cell bodies (indicated in a). (c) Fluorescent image of a transverse midbrain section from an owl in which a fluorescent tracer (dextran tetramethyl rhodamine, red) was injected iontophoretically into the Imc. The section was also stained for inhibitory neurons using an antibody to both GAD65 and GAD67 (green). Yellow somata indicate double-labeled (red and green) Imc neurons. Note the sparseness of Imc neurons.

inhibitor of ionotropic glutamate receptors, delivered through a multi-barreled recording and injection electrode, positioned at specific sites in the Imc space map (Online Methods).

Role of the Imc in exogenous competitive inhibition

We first tested the hypothesis that the Imc circuit mediates stimulus-driven (exogenous) competitive inhibition in the midbrain network. Exogenous, competitive inhibition in the OTid exhibits several distinctive properties: it operates across the entire space map, acts independently of the modality of the stimulus and the strength of the inhibition increases as the strength of the competitor is increased. These properties can only be observed when multiple stimuli are presented to the animal[11,13]. In our experiments, we measured them by simultaneously presenting two stimuli to the owl: one centered in the receptive field (RF) of the OTid unit (RF stimulus) and the other (competitor) located far outside of the RF, typically >30° from the RF center. The RF stimulus was always a visual looming dot and the competitor was either another looming dot or an auditory noise burst (Online Methods).

We began by measuring the contribution of the Imc to the suppressive effect of a distant competitor on spatial tuning curves in the OTid (Fig. 2a–i). Consistent with past results[11], the competing stimulus strongly suppressed OTid unit responses to an RF stimulus (Fig. 2d,g). We then positioned the iontophoretic electrode at the site in the Imc space map that represented the location of the competitor (Fig. 2b). Ejection of kynurenic acid blocked all responses to the competitor at the Imc injection site (Fig. 2j,k). At the same time, it also abolished competitor-mediated inhibition in the OTid (Fig. 2d,e,g,h). Following cessation of Imc blockade, responses to the competitor in the Imc and competitive inhibition in the OTid both re-appeared (Fig. 2f,i,l). Moreover, responses to RF stimuli presented alone remained unchanged across the three conditions (maximum response to RF stimulus alone during baseline versus Imc blockade: t test, $t_{22} = 2.99$, $P = 0.233$; maximum response to RF stimulus alone during Imc blockade versus recovery: Wilcoxon ranksum test, $Z = 0.03$, $P = 0.98$; Fig. 2g–i).

We verified these effects across a population of 18 OTid units (Fig. 2m,n and Supplementary Fig. 1). Powerful competitive suppression during the baseline condition (Fig. 2m) was abolished for the majority of units following Imc blockade (16 of 18 units; Fig. 2m and Supplementary Fig. 1b). Responses to single stimuli, however, remained unaffected for the majority of units (14 of 18; Supplementary Fig. 1c). The RF locations of the tested units and, thus, the positions of the competitor stimuli, were distributed widely across space (median distance of competitor from RF center = 43°; median loom speeds: RF stimulus, 4° s^{-1}; competitor, 7.2° s^{-1}; Supplementary Fig. 1d), demonstrating the Imc's role in mediating exogenous suppression across the entire OTid space map. The variability in the strength of competitive suppression in the baseline condition (Fig. 2m) did not correlate with the spatial positions of the competitors

($P > 0.05$, individual factors and two-factor interaction; two-way ANOVA on the percentage of suppression in the baseline condition with azimuthal and elevational distances as factors, $n = 18$ units from 4 birds; azimuth: $F_{1,14} = 0.28$, $P = 0.6$; elevation: $F_{1,14} = 0.38$, $P = 0.55$; interaction: $F_{1,14} = 0.28$, $P = 0.61$). Instead, the variability was consistent with unit-to-unit variability in the strength of competitive suppression, as reported previously[11,13].

The elimination of competitive inhibition in the OTid by Imc blockade occurred only when the competitor was positioned at the location represented at the site of blockade in the Imc space map. When the competing stimulus was moved away from the locus represented at the Imc inactivation site (median separation = 30°; Supplementary Fig. 2a), but still outside of the OTid RF (Fig. 3a), Imc blockade had no effect on competitor suppression of OTid responses (Fig. 3a). This result indicates that sensory input to the Imc circuit is spatially precise and that our blockade of Imc drive was focal.

Next, we tested whether the Imc mediates exogenous competitive inhibition across sensory modalities. To address this question, we repeated the first experiment, but replaced the visual competitor with an auditory competitor (Fig. 3b). The auditory competitor was a broadband noise burst with a median binaural level of 42 dB above unit threshold and located, in dichotic space, 38 ± 2° to the side of the OTid RF center (Supplementary Fig. 2c). The binaural level (strength) of the auditory competitor was chosen to yield consistently strong competitive inhibition across OTid units, based on results from a previous study[13]. As expected, a distant auditory competitor powerfully suppressed OTid unit responses to the visual RF stimulus ($n = 14$; Fig. 3b). This cross-modal suppression was, again, markedly reduced by focal blockade at the Imc site that represented the location of the auditory stimulus (Fig. 3b and Supplementary Fig. 2d).

Finally, we tested whether the unusual strength dependence of competitive inhibition in the OTid depends on the Imc[13,15]. For most units in the OTid, inhibition by a distant competitor increases with the strength of the competitor[13] (the others are not affected by a competitor). Notably, for half of these units, the inhibition increases abruptly, in a switch-like manner, when the strength of the competitor exceeds that of the RF stimulus; for the other half, inhibition increases gradually with the strength of the competitor stimulus. When the responses of switch-like, gradual and non-suppressed units are examined together, the resulting pattern of population activity exhibits abrupt changes as a function of relative stimulus strength, and categorizes stimuli as 'strongest' or 'other'.
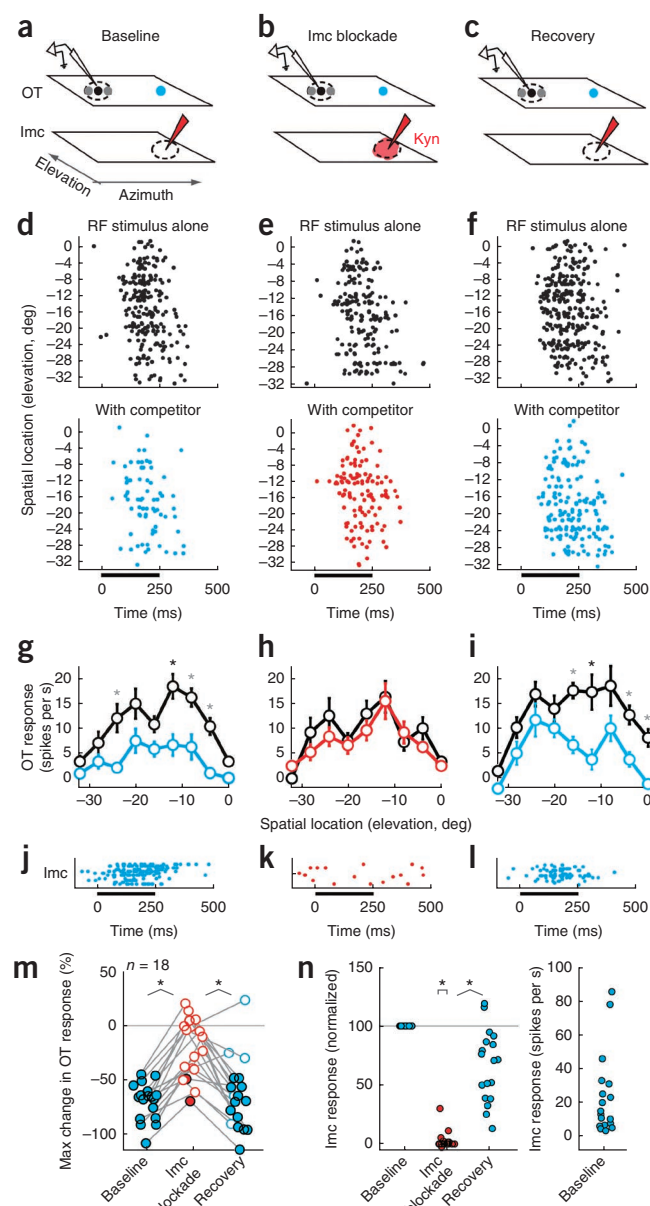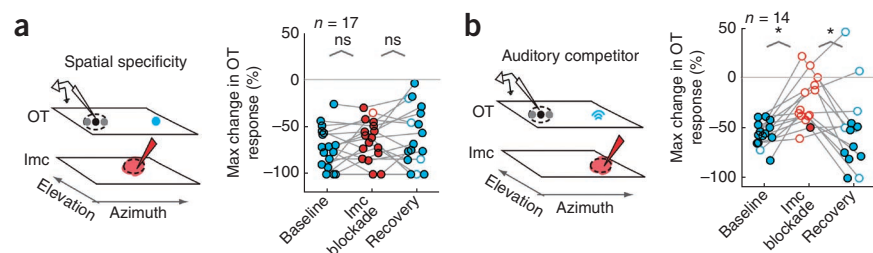
To test the role of the Imc in mediating this competitor strength-dependent inhibition, we measured competitor strength-response profiles with and without Imc blockade (Fig. 4a). For these experiments, the RF stimulus was presented with a fixed strength (average loom speed = 7 ± 0.8° s^{-1}) at the center of the OTid RF, and the distant competitor (median distance from RF center = 42°; Supplementary Fig. 2e)

Figure 2 Exogenous competitive inhibition in the OTid abolished by Imc blockade. (**a–c**) Schematics of electrode configurations for baseline, Imc blockade and recovery conditions. Illustrated are the space maps encoded in the OTid and Imc, receptive fields (dashed ovals: RFs), locations of visual stimuli (black and gray dots: RF stimulus; blue dot: competitor), and electrodes (recording in the OTid; recording/iontophoresis in the Imc). Dot size indicates strength of the stimulus; competitor was always stronger than RF stimulus. Red shading in **b** indicates drug being ejected. Kyn, kynurenic acid. (**d–f**) Rasters of spike responses of an OTid unit to the RF stimulus alone (top) or to the RF stimulus and distant competitor (bottom). Bar indicates stimulus duration. The distance between the OTid RF and the location of the competitor (also the site of Imc inactivation) was 33° (loom speeds: RF stimulus = 4° s^{-1}, competitor = 7.2° s^{-1}). (**g–i**) Responses (firing rates) of the OTid unit to the RF stimulus alone (black), or to the RF stimulus and distant competitor (blue or red). Data represent mean ± s.e.m. Gray and black asterisks indicate $P < 0.05$, t tests at individual locations followed by Holm-Bonferroni correction ($n = 12$ reps per stimulus condition per location, degrees of freedom = 22; see Online Methods). Black asterisks also indicate maximum suppression. (**j–l**) Rasters of Imc unit responses to the competitor stimulus at the site of drug injection. Dots represent individual spikes and rows represent different stimulus repetitions. (**m**) Population summary of maximum response suppression of OTid units (circles) by a distant competitor. Maximum suppression for each unit typically occurred at or near the unit's RF center. Filled circles indicate that maximum suppression was significant ($P < 0.05$, tested as in **g**), and open circles indicate that it was not significant ($P > 0.05$, as in **h**). Gray lines connect responses of one unit across conditions. Horizontal spread of points in each condition represent random jitter to improve visualization of individual points. *$P < 0.05$, paired Wilcoxon sign rank tests followed by Holm-Bonferroni correction (baseline versus blockade, $Z = -3.72$, $P = 2 \times 10^{-4}$; blockade versus recovery, $Z = -3.42$, $P = 6 \times 10^{-4}$; $n = 18$ units from 4 birds; also see **Supplementary Fig. 1a,b**). (**n**) Population summary of Imc unit responses to the competitor at the site of blockade. Left, response normalized by firing rate in the baseline condition. *$P < 0.05$ (blockade versus 100, Wilcoxon sign rank test, $Z = -3.82$, $P = 1 \times 10^{-4}$; blockade versus recovery, paired Wilcoxon sign rank test, $Z = -3.72$, $P = 2 \times 10^{-4}$; $n = 18$ units from 4 birds). Right, absolute firing rates of Imc units.

was presented over a range of (interleaved) strengths (**Supplementary Fig. 2e** and ref. 13). Imc blockade at the site that represented the location of the competitor abolished the competitor strength–dependent inhibition: responses to the RF stimulus were no longer correlated with the strength of the competitor, and the maximum suppression (typically caused by the strongest competitor; $17 \pm 1°$ s^{-1}) was not substantially different from zero (**Fig. 4b,c**). We verified these effects across a population of OTid units ($n = 7$ switch-like and 5 gradual units; **Fig. 4d–f** and **Supplementary Fig. 2f**). Thus, the Imc mediates competitor strength–dependent, exogenous inhibition in the OTid, and is therefore necessary for constructing a categorical representation of the strongest stimulus in the OTid.

Role of the Imc in endogenous competitive inhibition

Next, we tested the hypothesis that the Imc circuit also mediates the competitive inhibition that is associated with endogenous signals.

Figure 3 The Imc mediates space-specific, sensory modality–independent and switch-like exogenous competitive inhibition in the OTid. (**a**) Spatial specificity. Left, the competitor stimulus was located outside both the OTid and Imc RFs. Right, population summary of competitive suppression of OTid unit responses. Data are presented as in **Figure 2m**. ns, not significant ($P > 0.05$, paired t tests; baseline versus blockade, $t_{16} = -1.58$, $P = 0.14$; blockade versus recovery, $t_{16} = -0.65$, $P = 0.52$; $n = 17$ units from 4 birds). (**b**) Sensory modality independence. Left, blue icon denotes an auditory competitor stimulus. Right, population summary of the competitive suppression of OTid unit responses. Data are presented as in **Figure 2m**. *$P < 0.05$ (paired t tests followed by Holm-Bonferroni correction; baseline versus blockade, $t_{13} = -4.45$, $P = 0.0007$; blockade versus recovery, $t_{13} = 2.89$, $P = 0.013$; $n = 14$ units from 4 birds; also see **Supplementary Fig. 2d**).
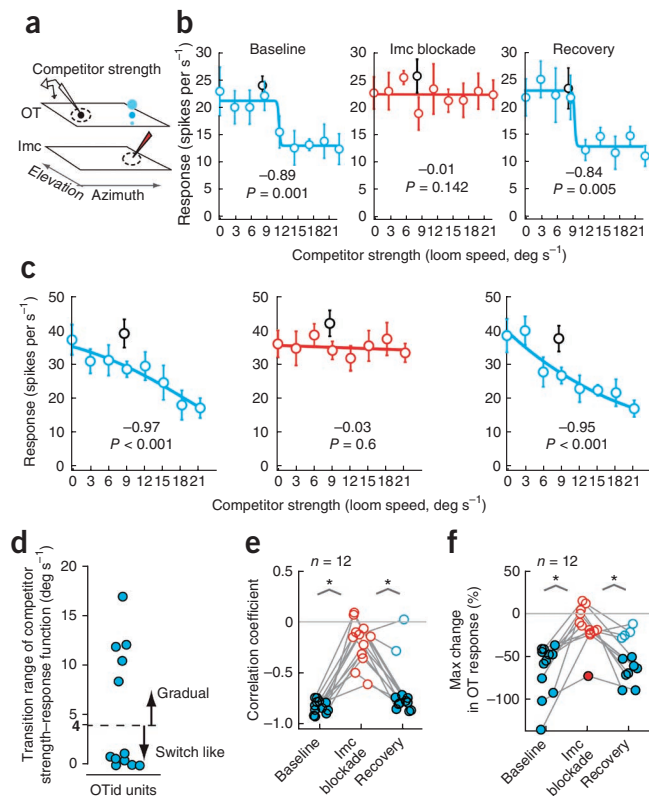
Figure 4 The Imc mediates competitor strength–dependent exogenous inhibition in the OTid. (**a**) Measurement of competitor strength–dependent response profiles. The strength of the competitor stimulus was systematically increased (blue dots of increasing sizes) while that of the RF stimulus was maintained constant (black dot). Data are presented as in **Figure 2a–c**. (**b**) Abrupt, switch-like increase in the suppression of an OTid unit's responses as competitor strength increased. Data represent ± s.e.m. Transition range = 0.6° s[−1] (left, Online Methods). Data in black show responses to RF stimulus alone. Correlation coefficients (response versus competitor strength) are indicated (Spearman test). (**c**) Gradual increase in the suppression of a different OTid unit's responses as competitor strength increased (Online Methods). Data represent ± s.e.m. Transition range = 16.8° s[−1] (left). (**d**) Distribution of transition ranges of competitor strength–dependent response profiles measured as in **a** (Online Methods). Using previously published criterion[13] for identifying switch-like versus gradual response profiles (a transition range cut off of 4° s[−1]), seven competitor strength–dependent response profiles were switch like and five were gradual. (**e**) Population summary of competitive response correlation coefficient. Data are presented as in **Figure 2m**. *$P < 0.05$ (paired t tests followed by Holm-Bonferroni correction; baseline versus blockade, $t_{11} = -9.6$, $P < 0.0001$; blockade versus recovery, $t_{11} = 5.4$, $P = 0.0002$; $n = 12$ units from 6 birds, 7 with switch-like increase in suppression and 5 with a gradual increase[13]; also see **Supplementary Fig. 2f**). (**f**) Population summary of maximum response suppression for same units. *$P < 0.05$ (paired Wilcoxon rank sum tests followed by Holm-Bonferroni correction; baseline versus blockade, $Z = -3.1$, $P = 0.002$; blockade versus recovery, $Z = -2.12$, $P = 0.034$).

To evoke space-specific endogenous signals, we applied sub-saccadic electrical microstimulation (currents weaker than those necessary to elicit eye movements, <30 μA) to the forebrain gaze control area, the arcopallial gaze field (AGF). The AGF shares many properties with the mammalian frontal eye field (FEF): similar patterns of anatomical projections to sensorimotor and premotor structures[20,21], a necessary role in working memory–dependent gaze control[22,23], changes in gaze direction caused by electrical microstimulation[20,24], and space-specific modulation of sensory neural responses caused by sub-saccadic electrical microstimulation[12,25]. In monkeys, such sub-saccadic microstimulation of the FEF evokes an endogenous signal that shifts spatial attention covertly to the locus encoded at the FEF stimulation site[26].

We applied sub-saccadic electrical microstimulation to the AGF while monitoring OTid responses to sensory stimuli. For these experiments,

we chose OTid sites that encoded locations that were distant from the one encoded by the AGF site (non-aligned OTid sites; average distance between OTid and AGF RFs = 34 ± 3.3°; **Fig. 5a–c** and **Supplementary Fig. 3g**). Consistent with previously published results[12], we found that AGF microstimulation produced a suppression of responses of non-aligned OTid units to sensory stimuli, with response suppression occurring predominantly at stimulus locations that were either at or near the center of the OTid RF (**Fig. 5d** and **Supplementary Fig. 3d**). We then positioned the iontophoresis electrode at the site in the Imc space map that encoded the same location as the AGF microstimulation site (aligned site; average distance between RFs = 2.2 ± 0.3°). Blockade of responses at the Imc site aligned with the AGF stimulation site completely abolished endogenous competitive inhibition (**Fig. 5e** and **Supplementary Fig. 3e**), and cessation of drug application resulted in recovery of endogenous competitive inhibition in the OTid (**Fig. 5f** and **Supplementary Fig. 3f**). This result was confirmed across a population of 14 OTid units, for which the site of Imc blockade was aligned with the AGF microstimulation site (**Fig. 5g** and **Supplementary Fig. 3h**). Note that, in this protocol, the endogenous signal encoded a location at which no stimulus was present[12,27,28].

Figure 5 Endogenous competitive inhibition in the OTid abolished by Imc blockade. (**a–c**) Schematics of the electrode configurations. Data are presented as in **Figure 2a–c**. Also shown is the AGF, with the blue lightning bolt signifying the locus of electrical microstimulation in the AGF (endogenous signal). (**d–f**) Responses of an OTid unit to the RF stimulus alone (black) or to the RF stimulus paired with AGF microstimulation at a non-aligned site (blue or red). Distance between the RFs of the OTid and AGF sites = 34°; distance between the RFs of the AGF site and the site of Imc inactivation = 2.5°; loom speed of RF stimulus = 5.6° s[−1]; strength of microstimulation current = 10 μA. Data represent mean ± s.e.m. Filled circles indicate responses to the stimulus location yielding maximal change; *$P < 0.05$, t tests at individual locations followed by Holm-Bonferroni correction ($n = 10$ repetitions per stimulus condition per location, degrees of freedom = 18; Online Methods). (**g**) Population summary of endogenous response suppression in the OTid, based on the maximum suppression obtained during a spatial tuning curve measurement for each unit (circles). Data are presented as in **Figure 2m**. *$P < 0.05$ (paired t tests followed by Holm-Bonferroni correction; baseline versus blockade, $t_{13} = -6.8$, $P < 0.0001$; blockade versus recovery, $t_{13} = 5.3$, $P = 0.0002$; $n = 14$ units from 5 birds; **Supplementary Fig. 3h**).
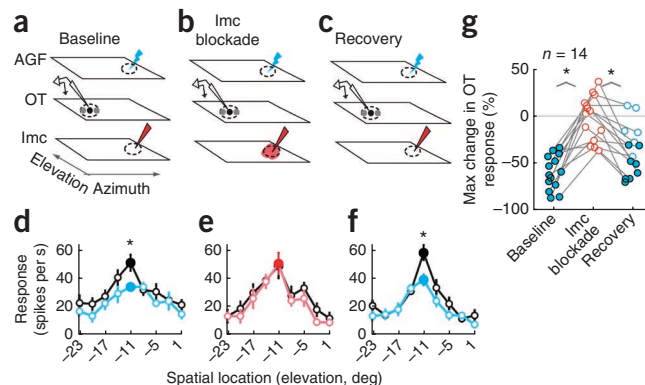
Figure 6 The Imc mediates space-specific, sensory modality–independent endogenous competitive inhibition in the OTid. (**a**) Spatial specificity. Top, the Imc RF is offset with respect to the AGF site, as well as the OTid site. Bottom, population summary of endogenous response suppression in the OTid. Data are presented as in **Figures 3a** and **5g**. ns indicates not significant, $P > 0.05$ (Mann-Whitney U tests, small sample size; baseline versus blockade, $P = 0.20$; blockade versus recovery, $P = 0.28$; $n = 8$ units from 4 birds). (**b**) Sensory modality independence. Top, black and gray icons represent the locations of an auditory RF stimulus. Bottom, population summary of endogenous response suppression in the OTid. Data are presented as in **Figure 5g**. *$P < 0.05$ (Mann-Whitney U tests followed by Holm-Bonferroni correction; baseline versus blockade, $P < 0.0001$; blockade versus recovery, $P = 0.014$; $n = 9$ units from 2 birds; **Supplementary Fig. 4d**).

This protocol is ideal for isolating the neural circuits responsible for endogenous competitive inhibition: the absence of a stimulus at the location encoded by the microstimulation site eliminates the explicit contribution of stimulus-driven, exogenous competitive inhibition.
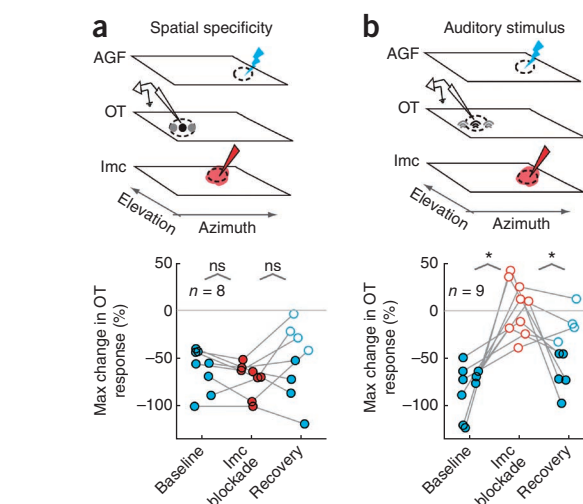
In other experiments, the Imc was blocked at sites that were non-aligned with both the AGF microstimulation site (average distance between RFs = $35 \pm 7.1°$) and the OTid unit RF (average distance = $42 \pm 6.5°$; **Fig. 6a** and **Supplementary Fig. 4a**). In this configuration, Imc blockade had no effect on endogenous competitive inhibition in the OTid (**Fig. 6a**), demonstrating the spatial specificity of the effects of Imc blockade on endogenous competitive inhibition (consistent with the effects of Imc blockade on exogenous competitive inhibition; **Fig. 3a**).

Finally, we tested whether endogenous competitive inhibition of auditory responses also depended on the Imc circuit. We repeated the experiment described above, but we replaced the visual RF stimulus with an auditory RF stimulus (**Fig. 6b** and **Supplementary Fig. 4c**). AGF microstimulation suppressed auditory responses at non-aligned sites in the OTid space map (**Fig. 6b**). Following Imc blockade at a site aligned with the AGF stimulation site, endogenous competitive inhibition of auditory responses in the OTid was eliminated (**Fig. 6b** and **Supplementary Fig. 4d**). Taken together, these results suggest that the Imc is required for generating competitive inhibition among both endogenous and exogenous signals in the OTid.

DISCUSSION

We found that a single, shared circuit in the midbrain selection network mediates competitive inhibition among both exogenous and endogenous signals. Global competitive inhibition caused by physically salient stimuli (exogenous competitive inhibition) has been reported for several brain areas, including prefrontal, parietal and extrastriate cortices in mammals[29–32] and in the OTid/superior colliculus of many species[16]. In addition, suppression of neural responses to task-irrelevant stimuli (endogenous competitive inhibition) has been documented in a similarly wide range of brain areas, mostly in primate species[17,33,34]. However, the Imc is the first circuit to be identified as mediating this critical function. The degree to which activity that is generated in the midbrain network modulates sensory responses in other brain areas remains to be determined.

The small population of GABAergic Imc neurons (<4% of the number of cells in layer 13 of the optic tectum; Online Methods) controlled competitive interactions across the entire OTid space map. By mediating this function across both exogenous and endogenous signals, the Imc circuit renders a representation of stimulus priority in the OTid. Moreover, because of switch-like competitive inhibition, the Imc circuit creates a categorical representation of the highest priority stimulus in the OTid, one that is exquisitely sensitive to the difference between the strengths of multiple competing stimuli. The observation that inactivation of the superior colliculus severely impairs the

ability of monkeys to select a stimulus either for gaze or attention, particularly when it is in the presence of similar competitors[9,10,35,36], suggests that the midbrain network, and specifically the Imc (or its homolog in mammals), is critical under these conditions. It will be important to assay the effect of inactivating the Imc or its analog[7] in animals that must select a target among similar distractors.

Given the essential role of the Imc in competitive inhibition in the midbrain network, several questions remain regarding the routing of information through the network. First, how do endogenous signals from the AGF activate the Imc? To date, the only known anatomical input to the Imc originates from the optic tectum[18]. Endogenous signals could be routed to the Imc via the optic tectum or via an unknown descending pathway. Second, what is the route by which Imc output suppresses neural responses in the OTid? This could be accomplished either directly, via the projections from the Imc to the OTid, and/or indirectly, via projections from the Imc to the nucleus isthmi pars parvocellularis (Ipc), a cholinergic nucleus with point-to-point, recurrent connections with the optic tectum. Imc inhibition of Ipc activity would reduce any amplifying effect that the Ipc may have on tectal unit responses[37]. The relative importance of these two pathways for OTid suppression needs to be examined. Finally, how do competitive signals in one brain hemisphere reach the opposite hemisphere? Here, both the exogenous and endogenous competitive signals were selected to correspond to locations that were explicitly represented on the same side of the brain as the RF stimulus (**Supplementary Figs. 1**–**4**). However, we have shown previously that stimulus locations that are explicitly represented only in opposite hemispheres can still be mutually inhibitory[11]. Whether cross-hemispheric inhibition is also mediated by the Imc remains an intriguing question.

Circuit-level models of the modulation of cortical activity by attention have proposed that endogenous signals modulate neural responses by operating through the same neural mechanisms that govern exogenous stimulus interactions[38–40]. Our results provide direct evidence in support of this hypothesis. Inhibitory circuits that act globally across spatial locations, such as the Imc, could explain interactions observed in the forebrain between remote stimuli competing for attention[39]. Moreover, Imc-like circuits acting globally across feature values (for example, orientation of visual contours, colors, etc.) could account for many of the local, normalizing sensory interactions and the effects of endogenously controlled attention on feature processing that have been reported in forebrain networks[39,41].

Numerous studies in monkeys and humans have established that neural responses to a sensory stimulus are stronger when an animal attends to the location of a stimulus than when it attends away from

that location[33,42,43]. Recent neuroimaging results from humans engaged in endogenous control of attention have suggested that these attention-dependent changes in neural responsiveness involve two distinct processes[44]: one that increases neural responses to the attended stimulus (focally) and another that suppresses neural responses to irrelevant information (globally). In support of distinct processes for enhancement and suppression, neurophysiological data from the owl midbrain selection network has shown that space-specific endogenous signals simultaneously generate both focal enhancement of sensory responses to stimuli at the corresponding location in the OTid space map and global suppression of sensory responses to stimuli at all other locations[45]. We found that the Imc contributes to global suppression. What circuits might underlie focal enhancement? In the avian midbrain network, the cholinergic Ipc with its recurrent connectivity with the optic tectum stands out as an excellent candidate. It will be important to determine whether the Ipc is, indeed, involved in focal response enhancement in the midbrain, what circuits serve this function in the forebrain, and whether focal enhancing circuits are also shared by both exogenous and endogenous signals.

METHODS
Methods and any associated references are available in the online version of the paper.

Note: Supplementary information is available in the online version of the paper.

AUTHOR CONTRIBUTIONS
S.P.M. and E.I.K. designed the study and wrote the paper. S.P.M. performed the experiments and the analyses.

COMPETING FINANCIAL INTERESTS
The authors declare no competing financial interests.

1. Fecteau, J.H. & Munoz, D.P. Salience, relevance, and firing: a priority map for target selection. *Trends Cogn. Sci.* **10**, 382–390 (2006).
2. Awh, E., Belopolsky, A.V. & Theeuwes, J. Top-down versus bottom-up attentional control: a failed theoretical dichotomy. *Trends Cogn. Sci.* **16**, 437–443 (2012).
3. Reynolds, J.H. & Chelazzi, L. Attentional modulation of visual processing. *Annu. Rev. Neurosci.* **27**, 611–647 (2004).
4. Bisley, J.W. The neural basis of visual attention. *J. Physiol.* (*Lond.*) **589**, 49–57 (2011).
5. Gazzaley, A., Cooney, J.W., Rissman, J. & D'Esposito, M. Top-down suppression deficit underlies working memory impairment in normal aging. *Nat. Neurosci.* **8**, 1298–1300 (2005).
6. McMains, S. & Kastner, S. Interactions of top-down and bottom-up mechanisms in human visual cortex. *J. Neurosci.* **31**, 587–597 (2011).
7. Knudsen, E.I. Control form below: the contribution of a midbrain network to spatial attention. *Eur. J. Neurosci.* **33**, 1961–1972 (2011).
8. Zanto, T.P. & Gazzaley, A. Neural suppression of irrelevant information underlies optimal working memory performance. *J. Neurosci.* **29**, 3059–3066 (2009).
9. Lovejoy, L.P. & Krauzlis, R.J. Inactivation of primate superior colliculus impairs covert selection of signals for perceptual judgments. *Nat. Neurosci.* **13**, 261–266 (2010).
10. McPeek, R.M. & Keller, E.L. Deficits in saccade target selection after inactivation of superior colliculus. *Nat. Neurosci.* **7**, 757–763 (2004).
11. Mysore, S.P., Asadollahi, A. & Knudsen, E.I. Global inhibition and stimulus competition in the owl optic tectum. *J. Neurosci.* **30**, 1727–1738 (2010).
12. Winkowski, D.E. & Knudsen, E.I. Top-down gain control of the auditory space map by gaze control circuitry in the barn owl. *Nature* **439**, 336–339 (2006).
13. Mysore, S.P., Asadollahi, A. & Knudsen, E.I. Signaling of the strongest stimulus in the owl optic tectum. *J. Neurosci.* **31**, 5186–5196 (2011).
14. Basso, M.A. & Wurtz, R.H. Modulation of neuronal activity by target uncertainty. *Nature* **389**, 66–69 (1997).
15. Mysore, S.P. & Knudsen, E.I. Flexible categorization of relative stimulus strength by the optic tectum. *J. Neurosci.* **31**, 7745–7752 (2011).
16. Mysore, S.P. & Knudsen, E.I. The role of a midbrain network in competitive stimulus selection. *Curr. Opin. Neurobiol.* **21**, 653–660 (2011).
17. Carrasco, M. Covert attention increases contrast sensitivity: psychophysical, neurophysiological and neuroimaging studies. *Prog. Brain Res.* **154**, 33–70 (2006).
18. Wang, Y., Major, D.E. & Karten, H.J. Morphology and connections of nucleus isthmi pars magnocellularis in chicks (*Gallus gallus*). *J. Comp. Neurol.* **469**, 275–297 (2004).
19. Marín, G. *et al.* A cholinergic gating mechanism controlled by competitive interactions in the optic tectum of the pigeon. *J. Neurosci.* **27**, 8112–8121 (2007).
20. Knudsen, E.I., Cohen, Y.E. & Masino, T. Characterization of a forebrain gaze field in the archistriatum of the barn owl: microstimulation and anatomical connections. *J. Neurosci.* **15**, 5139–5151 (1995).
21. Stanton, G.B., Goldberg, M.E. & Bruce, C.J. Frontal eye field efferents in the macaque monkey. II. Topography of terminal fields in midbrain and pons. *J. Comp. Neurol.* **271**, 493–506 (1988).
22. Knudsen, E.I. & Knudsen, P.F. Disruption of auditory spatial working memory by inactivation of the forebrain archistriatum in barn owls. *Nature* **383**, 428–431 (1996).
23. Dias, E.C. & Segraves, M.A. Muscimol-induced inactivation of monkey frontal eye field: effects on visually and memory-guided saccades. *J. Neurophysiol.* **81**, 2191–2214 (1999).
24. Bruce, C.J., Goldberg, M.E., Bushnell, M.C. & Stanton, G.B. Primate frontal eye fields. II. Physiological and anatomical correlates of electrically evoked eye movements. *J. Neurophysiol.* **54**, 714–734 (1985).
25. Moore, T. & Armstrong, K.M. Selective gating of visual signals by microstimulation of frontal cortex. *Nature* **421**, 370–373 (2003).
26. Moore, T. & Fallah, M. Control of eye movements and spatial attention. *Proc. Natl. Acad. Sci. USA* **98**, 1273–1276 (2001).
27. Sundberg, K.A., Mitchell, J.F. & Reynolds, J.H. Spatial attention modulates center-surround interactions in macaque visual area v4. *Neuron* **61**, 952–963 (2009).
28. Kastner, S., Pinsk, M.A., De Weerd, P., Desimone, R. & Ungerleider, L.G. Increased activity in human visual cortex during directed attention in the absence of visual stimulation. *Neuron* **22**, 751–761 (1999).
29. Falkner, A.L., Krishna, B.S. & Goldberg, M.E. Surround suppression sharpens the priority map in the lateral intraparietal area. *J. Neurosci.* **30**, 12787–12797 (2010).
30. Bair, W., Cavanaugh, J.R. & Movshon, J.A. Time course and time-distance relationships for surround suppression in macaque V1 neurons. *J. Neurosci.* **23**, 7690–7701 (2003).
31. Schall, J.D., Hanes, D.P., Thompson, K.G. & King, D.J. Saccade target selection in frontal eye field of macaque. I. Visual and premovement activation. *J. Neurosci.* **15**, 6905–6918 (1995).
32. Desimone, R., Moran, J., Schein, S.J. & Mishkin, M. A role for the corpus callosum in visual area V4 of the macaque. *Vis. Neurosci.* **10**, 159–171 (1993).
33. Desimone, R. & Duncan, J. Neural mechanisms of selective visual attention. *Annu. Rev. Neurosci.* **18**, 193–222 (1995).
34. Knudsen, E.I. Fundamental components of attention. *Annu. Rev. Neurosci.* **30**, 57–78 (2007).
35. Nummela, S.U. & Krauzlis, R.J. Inactivation of primate superior colliculus biases target choice for smooth pursuit, saccades and button press responses. *J. Neurophysiol.* **104**, 1538–1548 (2010).
36. Zénon, A. & Krauzlis, R.J. Attention deficits without cortical neuronal deficits. *Nature* **489**, 434–437 (2012).
37. Marín, G., Mpodozis, J., Sentis, E., Ossandon, T. & Letelier, J.C. Oscillatory bursts in the optic tectum of birds represent re-entrant signals from the nucleus isthmi pars parvocellularis. *J. Neurosci.* **25**, 7081–7089 (2005).
38. Lee, D.K., Itti, L., Koch, C. & Braun, J. Attention activates winner-take-all competition among visual filters. *Nat. Neurosci.* **2**, 375–381 (1999).
39. Reynolds, J.H. & Heeger, D.J. The normalization model of attention. *Neuron* **61**, 168–185 (2009).
40. Lee, J. & Maunsell, J.H. A normalization model of attentional modulation of single unit responses. *PLoS ONE* **4**, e4651 (2009).
41. Cavanaugh, J.R., Bair, W. & Movshon, J.A. Nature and interaction of signals from the receptive field center and surround in macaque V1 neurons. *J. Neurophysiol.* **88**, 2530–2546 (2002).
42. Kastner, S. & Ungerleider, L.G. Mechanisms of visual attention in the human cortex. *Annu. Rev. Neurosci.* **23**, 315–341 (2000).
43. Carrasco, M. Visual attention: the past 25 years. *Vision Res.* **51**, 1484–1525 (2011).
44. Gazzaley, A., Cooney, J.W., McEvoy, K., Knight, R.T. & D'Esposito, M. Top-down enhancement and suppression of the magnitude and speed of neural activity. *J. Cogn. Neurosci.* **17**, 507–517 (2005).
45. Winkowski, D.E. & Knudsen, E.I. Distinct mechanisms for top-down control of neural gain and sensitivity in the owl optic tectum. *Neuron* **60**, 698–708 (2008).

ONLINE METHODS

Animals. Experiments were performed on nine head-fixed, non-anesthetized, adult barn owls (*Tyto alba*). Both male and female birds were used. All procedures for bird care and use were approved by the Stanford University Institutional Animal Care and Use Committee and were in accordance with the US National Institutes of Health and the Society for Neuroscience guidelines for the care and use of laboratory animals. Owls were group housed in enclosures in the vivarium, each containing 3–5 birds. The light/dark cycle was 12 h/12 h.

Neurophysiology. Experiments were performed as described previously[11,13,46]. Briefly, epoxy-coated tungsten microelectrodes (A-M Systems, 250 µm, 5 MΩ at 1 kHz) were used to record single and multi-units extracellularly. A mixture of isofluorane (1.5–2%, vol/vol) and nitrous oxide/oxygen (45:55 by volume) was used at the start of the experiment to anesthetize the bird and secure it in the experimental rig (a 20-min period of initial set-up). Isofluorane was turned off immediately after the bird was secured and was not turned back on for the remainder of the experiment. Frequently, nitrous oxide was also turned off at this point, but was left on for a few hours in several experiments if the bird's temperament necessitated it (some birds were calm when restrained, whereas others were not). However, it was turned off at least 30 min before the recording session. Our recordings were performed between 10 to 20 h after initial set-up (the time required for positioning the electrodes). Given that recovery from isofluorane occurs well under 30 min after it is turned off, and recovery from nitrous oxide occurs within a minute (the bird stands up and flies away if freed from restraints), recordings were made in animals that were not anesthetized.

Multi-unit spike waveforms were sorted off-line into putative single units, as described previously[13]. All recordings in the optic tectum were made in layers 11–13 of the optic tectum (OTid). Visual and auditory stimuli used here have been previously described[11,13]. Briefly, looming stimuli were dots that expanded linearly in size over time, starting from a size of 0.6° in radius. Visual stimuli were presented on a tangent screen in front of the owl. Auditory stimuli, delivered dichotically through matched earphones, were presented as though from different locations by filtering sounds with head-related transfer functions[47]. The average binaural levels (referred to also as sound levels) of auditory stimuli are indicated in all figures relative to the minimum threshold, averaged across units. The levels (strengths) of the auditory competitors were chosen to achieve powerful, substantial suppression of responses to the visual, looming RF stimulus (**Fig. 3b**; based on previous investigations[13]). No attempt was made to match the strengths of auditory competitors (**Fig. 3b**) with those of the visual competitors (**Fig. 2**) because such matching was not relevant to the question being asked. It was only important that the competitors be effective in suppressing responses to the RF stimuli.

In **Figures 2**, **3**, **5** and **6**, each RF stimulus location was repeatedly tested 10–15 times in a randomly interleaved fashion. Similarly, in **Figure 4**, each competitor strength value was repeatedly tested 10–15 times in a randomly interleaved fashion.

Iontophoretic blockade. Focal, reversible blockade of excitatory transmission was achieved by iontophoresing the fast onset/offset, pan–glutamate receptor antagonist kynurenic acid (Sigma, 40 mM, 8.5–9 pH), contained in one of the barrels of a three-barrel glass electrode (FHC, three-barrel borosilicate capillary tubing, 1.2- or 1.5-mm outer diameter for each barrel; tip diameter = 25–30 µm for all three barrels together). Ejection was achieved by passing approximately −500 nA through the drug barrel using a DAGAN 6400Adv iontophoresis amplifier. Data in the inactivation and recovery conditions were recorded 5–10 min after drug ejection started or after drug ejection ceased, respectively (by setting the retaining current to +15 nA). In all cases, the effects of drug onset/offset were verified by examining the responses of the Imc neurons at the site of inactivation. These responses were recorded using one of the other barrels of the glass electrode, which contained a carbon fiber and was saline filled; the third barrel (also saline filled, SUM channel) was used to balance the charge delivered by the kynurenic acid–containing barrel.

Following delivery of kynurenic acid to the Imc, stimulus-driven activity at that Imc site was almost completely abolished (**Fig. 2n**). This was further verified in a subset of sites by measuring responses to increasing strengths (loom speeds) of the competitor stimulus in the three conditions (data not shown). In some cases (~25%), the delivery of kynurenic acid resulted in the appearance of a large number of spikes that could not be driven by the competitor stimulus. These stimulus-insensitive spikes disappeared once the delivery of kynurenic acid ceased. As the Imc is replete with fibers of passage, and Imc neurons are thought to be mutually inhibitory[18,46], this increase in the number of stimulus-insensitive spikes measured at the inactivated site is best explained as the increased activity of fibers of passage from other Imc neurons that have been disinhibited due to synaptic blockade at the inactivated site.

AGF microstimulation. Electrical microstimulation of the AGF was achieved following the protocol described previously[12,48]. Briefly, an epoxy-coated tungsten microelectrode (FHC, 1 MΩ at 1 kHz) was used to identify a patch of tissue in the AGF with consistent spatial tuning. This was defined as a 300-µm span along the dorsoventral penetration path of the electrode, such that the locations of unit visual receptive fields measured at the top, middle and bottom of the span were not significantly different (centered within ±5°). Electrical stimulation consisted of biphasic 200-Hz pulses, delivered for 25 ms (Grass S88 stimulator with two Grass stimulus isolation units PSIU-6). AGF stimulation was delivered starting at 0 ms (that is, simultaneously with stimulus onset) when the RF stimulus in the OTid RF was visual, and at −25 ms (25 ms before stimulus onset) when the RF stimulus was auditory. Current levels (5-25 µA) were far below those required to elicit small amplitude eye deflections (100–600 µA); current amplitudes were measured from the voltage drop across a 1-kΩ resistor in the return path of the current source.

Data analysis and statistical methods. All analyses were carried out with custom MATLAB code. The spatial receptive field for each unit was defined as the set of locations at which a single stimulus evoked responses above baseline. The receptive field locations of the recorded units in the OTid, Imc and AGF are shown for each set of experiments in **Supplementary Figures 1c**, **2a,c,e**, **3g** and **4a,c**. Note that, in the barn owl, the OTid in each hemisphere represents locations from up to 15° into ipsilateral space (−15°) through 60° into contralateral space (+60°).

Response firing rates were computed by counting spikes over a time window and converting the resulting count into spikes per second. The optimal window for each unit was defined as the time between the first instant at which the inhibition was statistically significant, and the last instant at which it was statistically significant, after rounding off both values to the nearest multiple of 10 ms. Statistical significance was determined as described previously[13]. Briefly, we compared the average instantaneous firing rates obtained with the RF stimulus alone versus with both the RF stimulus and a competitor/AGF stimulation using a running ANOVA and an empirical criterion for significant difference at the 0.05 level[13]. For **Figures 2** and **3a**, the median start and end times of the windows were 50 ms and 300 ms, respectively, with stimulus onset occurring at 0 ms. The median count windows for the other experimental tests were 0 ms and 300 ms (**Figs. 3b** and **4b–f**), 110 ms and 310 ms (**Fig. 5**), 150 ms and 320 ms (**Fig. 6a**), and 50 ms and 230 ms (**Fig. 6b**), respectively. The differences in the windows reflected a combination of unit-to-unit variability in the onset and duration of inhibition, as well as the source dependence of the inhibitory signal (inhibition due to a visual versus an auditory stimulus, or an endogenous signal).

Parametric or nonparametric paired statistical tests were applied on the basis of whether the distributions being compared were Gaussian or not (Lilliefors test of normality); tests were always two-tailed. The Holm-Bonferroni correction for multiple comparisons was applied when appropriate by including only those comparisons that were individually significant. In statistically comparing the data across the three experimental conditions (baseline, Imc blockade and recovery), the experimenter was not blind to the experimental conditions to which the data sets belonged.

Correlations between responses to paired stimuli and the strength of the competitor stimulus were tested using Spearman's rank correlation coefficient (*corr* command in MATLAB with the Spearman option).

The transition range of a competitor strength-response profile was defined as the range of competitor strengths over which responses dropped from 90% to 10% of the total range of responses[13]. The range of responses was estimated by fitting sigmoidal functions to the data, and using the fits to determine the minimum and maximum response levels over a standard range of loom-speeds (0–22° s^{-1}). Switch-like response profiles were defined as those for which the transition range was ≤4° s^{-1} (ref. 13).

The OTid is approximately 6 mm rostrocaudally and 4.1 mm dorsoventrally after accounting for curvature. In contrast, the Imc is only 2.8 mm rostrocaudally and 0.35 mm dorsoventrally, appearing as a 700-µm × 350-µm elliptical disk in transverse sections (shown here). The numbers of cells in the Imc and layer 13 of the optic tectum were estimated by counting cell bodies in seven representative Nissl sections, and using the counts to calculate the total number of cells over the entire volumes of these structures.

Replicability. As demonstrated by the summary data in **Figures 2–6**, the experiments were all repeatable. However, because of the complexity of the design of the experiment in **Figures 5** and **6** (involving precise positioning of three electrodes, including one three-barrel glass electrode), and the length of each experiment (frequently >15 h), only about 40% of these experiments were successful. In the remaining attempts, the experiments were terminated after 15 h if data collection within a few hours did not appear feasible.

46. Mysore, S.P. & Knudsen, E.I. Reciprocal inhibition of inhibition: a circuit motif for flexible categorization in stimulus selection. *Neuron* **73**, 193–205 (2012).
47. Witten, I.B., Knudsen, P.F. & Knudsen, E.I. A dominance hierarchy of auditory spatial cues in barn owls. *PLoS ONE* **5**, e10396 (2010).
48. Winkowski, D.E. & Knudsen, E.I. Top-down control of multimodal sensitivity in the barn owl optic tectum. *J. Neurosci.* **27**, 13279–13291 (2007).